Nylon 6/CB Polymeric Conductive Plastic Bipolar Plates for PEM Fuel Cells

Chao-Kuang Chen, Jenn-Kun Kuo

Department of Mechanical Engineering, National Cheng Kung University, Tainan 70101, Taiwan

ABSTRACT: Bipolar plate materials are a potential alternative to the graphite sheets currently used in proton exchange membrane fuel cells (PEMFCs). These materials must be of low-cost, easy to fabricate, light, strong, mechanically stable, and have a low surface contact resistance if they are to be widely applicable. Nylon 6 polymer thermoplastic and carbon black (CB, 100–600 nm) blends have nanoparticle carbon (30–50 nm), high electrical and thermal conductivity, and good gas tightness properties. These composites are suitable for the mass fabrication of bipolar plates using an injection molding process. In this study, various Nylon 6/CB composites are used to fabricate bipolar-parallel-plate gas-flow channel. The bipolar plates are fabricated with three different gas flow channel configurations, namely serpentine, grid, and branch. The bipolar plates are then used in the construction of PEMFCs. The temperature effect on the resistivity of the Nylon 6/CB polymeric composite is investigated and the voltage–current curves and power density–current curves obtained from the different PEMFCs are analyzed. © 2006 Wiley Periodicals, Inc. J Appl Polym Sci 101: 3415–3421, 2006

Key words: bipolar plate; PEMFC; nylon 6 polymer thermoplastic; injection molding; nanoparticle carbon

INTRODUCTION

Proton exchange membrane fuel cells (PEMFCs) represent one of the most promising power sources in the near future for residential, mobile, and automobile applications. These fuel cells offer the advantages of compactness, lightweight, high power density, and a low temperature operation. However, the manufacturing costs of fuel cell stacks are high and limit their current commercial viability. Although catalyst loading and membrane thickness have both been successfully reduced in recent decades, material costs still pose a barrier to the wider commercialization of PEMFCs. Of the various components comprising a PEMFC device, the bipolar plates make the greatest contribution to the total stack cost. In fact, it has been reported that the graphite plates currently used in these devices account for ~60% of the total cost.[1] The target cost for bipolar plates designed for fuel cell-driven vehicles has been established as 25–50 $/kW.[2,3] The bipolar plate is a multifunctional component of the PEMFC. Its primary roles include delivering the reactant gases to the fuel cell electrodes, providing an electrical connection between adjacent cells in the stack, removing the water by-product from the cell, and transferring away reaction heat. A bipolar plate must meet the following material and construction requirements:[4]

1. good electrical conductivity;
2. good thermal conductivity;
3. gas tightness;
4. corrosion resistance in acid, with oxygen, heat, and humidity;
5. minimal volume and weight; and
6. inexpensive material and processing costs.

The high cost of graphite-based bipolar plates is because of the brittleness of the graphite, which drives the machining costs of the flow channels on the plates to prohibitively high levels. Accordingly, extensive research has been conducted to identify low-cost high-performance alternatives to graphite. Various candidate materials have been proposed, including metal-based bipolar plates,[5–7] carbon-filled polymers,[8] and carbon/carbon composites.[9] For materials with high carbon concentrations, injection molding provides the means to mass produce low-cost bipolar plates.[10] Injection and compression molding of carbon-filled polypropylene and polyphenylene sulfide were used to fabricate the bipolar plates. Loadings up to 60 wt % in the form of graphite, conductive carbon black, and carbon fibers were investigated.[11]

The carbon structure of nanotubes and nanostructures is one of very highly ordered graphite.[3] Template-synthesized carbon can be fabricated as free-standing nano-porous carbon membranes,[12] and narrower, highly ordered graphitic carbon nanotubes can be prepared within the membranes for electrochemical energy storage and production.[13] Both the

Correspondence to: C. K. Chen (ckchen@mail.ncku.edu.tw).

TABLE I
Nylon 6 Properties

Property	Test method	Value (unit)
Density at 25°C	ISO 1183	1128 (kg/m^3)
Hardness (15 s value)	ASTM 868	80 (Shore D)
Heat distortion temperature at 1.80 MPa	ISO 75	59 (°C)
Vicat softening point at 10 N	ISO 306	215 (°C)
Melt flow index (275°C/10 kg)	ISO 1133	43 (g/10 min)
Melt flow index (275°C/5 kg)	ISO 1133	9 (g/10 min)
Flexural modulus	ISO 178	2900 (MPa)
Flexural strength	ISO 178	7 (MPa)
Tensile strength at break	ISO 527	45 (MPa)
Tensile strength at yield	ISO 527	50 (MPa)
Elongation at break	ISO 527	15 (%)
Notched Izod impact at 23°C	ISO 180	8 (kJ/m^2)
Mold shrinkage	ASTM D-955	1.7–2.0 (%)
Volume resistivity	–	100 (ohm-cm)
Surface resistivity	–	10^3 (ohm/sq)
Degree of water absorption 23°C (in water) 24 h	–	1.8 (%)

outer and the inner tubules are electrochemically active and are suitable for the intercalation of lithium ions or fuel cells. The membranes can also be filled with nanoparticles of electocatalytic metals and alloys. Such catalyst-loaded membranes can be used to electrocatalyze O$_2$ reduction and methanol oxidation, two reactions of great importance in PEMFC technology.

It has been known that carbon black-filled thermoplastic composites exhibit both percolation phenomenon[14–16] and specific temperature dependence of resistivity.[17,18] The former makes the materials have a wide range of conductivity from insulator to semiconductor, depending on CB concentration. The latter is characterized by either positive temperature coefficient (PTC) effect or negative temperature coefficient. For a polymer-based PTC material of practical value, its volume resistivity increases remarkably by several orders of magnitude when temperature approaches the melting point of matrix resin.[19] In regard to the bipolar plate material selection, care should be taken in selecting a polymer matrix with solid–liquid phase transition that is far above the operating temperature of the fuel cell to avoid this conductivity loss.

EXPERIMENTAL

Preparation of PEM fuel cells

In this study, Nylon 6 (CABELEC-3178, Cabot) polymer thermoplastic material was chosen as the polymer matrix because of its low cost, electrical conductivity, gas tightness, chemical stability, good impermeability, favorable mechanical properties, and injection molding applications (Table I). The bipolar plates were fabricated from a material composing Nylon 6 polymer thermoplastic and carbon black and excellent conductivity nanoparticle carbon powder properties (Vulcan XC-72, Cabot) is shown in Table II. The weight percentage of each component is shown in Table III. In addition to the CB/Nylon6/carbon nanoparticles carbon, the bipolar plate material also included a small weight percentage of additional additives designed to increase its electrical conductivity, strength, and gas tightness.

Nylon 6 is a nonconductor, with good electronic conductivity and excellent corrosion resistance, and forms homogeneous mixtures when combined with suitable resins. Generally, the electrical properties and the mechanical stability of bipolar plates are improved with increased carbon content. Therefore, the present study specified a basic composition for the bipolar plates of 50–55 wt % Nylon 6 polymeric composite with adhesive, 35 wt % carbon black, and 10 wt % nanoparticle carbon powder. Using an injection molding process, bipolar plates were fabricated with a total thickness of 3.5 mm and an active area of 25 cm^2.

The membrane-electrode assembly (MEA) was fabricated by placing electrodes on either side of a pretreated Nafion 112 (50 μm) membrane (ElectroChem), with platinum loadings of 0.2 and 0.4 mg/cm^2 for the anode and cathode, respectively. A fuel cell was then constructed using the prepared MEA, a Teflon gasket, and two Nylon 6 flow-field plates positioned on either side of the MEA [see Fig. 1(a)].

TABLE II
Nanoparticle Carbon Powder Properties

Property	Test method	Value (unit)
Iodine number	ASTM D-1510	253 (mg/g)
OAN	ASTM D-2414	174 (cc/100 g)
325 mesh residue	ASTM D-1514	<25 (ppm)
Moisture as packed	ASTM D-1509	<1.0 (%)
Density	ASTM D-4820	264 (kg/m^2)
Particle size (avg.)	ASTM D-3849	30 (nm)

Component	(%)
Nylon 6 polymeric thermoplastic	50–55 wt %
Carbon black	35 wt %
Nanoparticle carbon	10 wt %

In this study, three different flow channel configurations were fabricated, namely serpentine, grid, and branch, as shown in Figure 2. The performance and characteristics of the fuel cells incorporating the three different gas channel configurations were thoroughly analyzed and compared.

Characterization of PEM fuel cells

The voltage–current (VI), power density–current (PI), and open circuit voltage (OCV) characteristics of the PEM fuel cells were obtained using a digital multimeter supplied by Bean 300M (Bean Co., Taiwan) [shown in Fig. 1(b)] linked to an IBM PC. The electrolyte was characterized using a scanning electron microscopy (SEM) technique (JSM-5610, JEOL). A sectional SEM photograph of the electrolyte was obtained to establish the quality of the Nylon 6 bipolar plates. The electrical properties of the polymer composite (e.g., its resistivity) were examined over the temperature range of 22–120°C, with the composite being heated by an attached heater.

Operation and performance evaluation of PEM fuel cells

As stated previously, this study fabricated PEM fuel cells with three different gas flow channel configurations, i.e., serpentine, grid, and branch. The aim of these flow channels is to ensure a uniform temperature and gas distribution in the Nylon 6 thermoplastic bipolar plates. At the beginning of the PEM fuel cell operation, humidified hydrogen and oxygen gases were supplied to the anode and the cathode of the fuel cell, respectively. The PEM fuel cells were operated at room temperature (25–30°C). The humidity of the pure hydrogen (99.999% H_2; 200 sccm) was varied from 10 to 100% during the OCV measurement, and maintained at 100% for all other measurements. Meanwhile, humidified oxygen gas (200 sccm) was supplied to the cathode side throughout all measurement operations.

The VI and PI characteristics were established for the fuel cells incorporating bipolar plates with the three different gas flow channel configurations. The measured resistance includes contributions from the bulk material and from the two contact resistances between the diffusion media and the plates. The
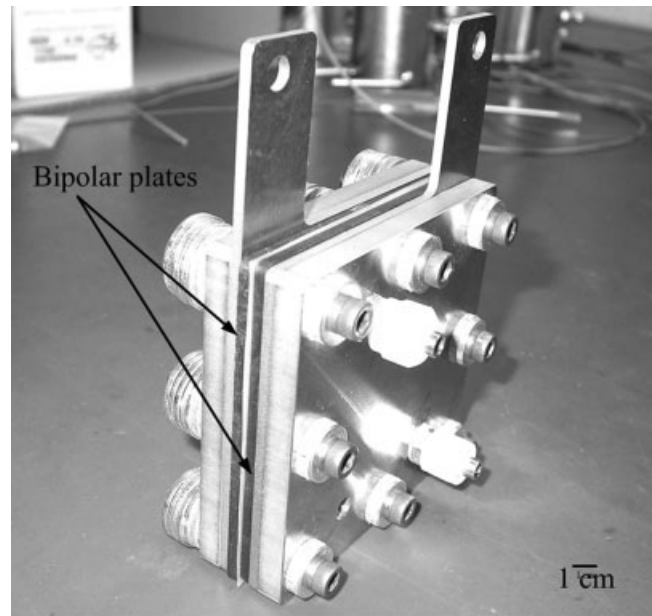
(a) Single PEM fuel cell
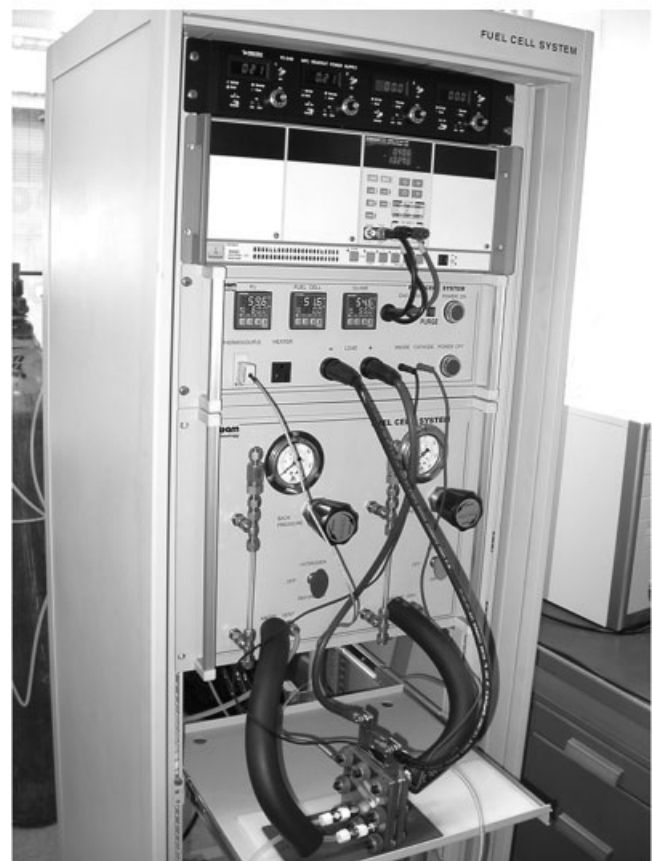
(b) Measurement system

Figure 1 Photographs of Bean 300M measurement system and Nylon 6 polymeric conductive plastic bipolar plates of single PEM fuel cell.
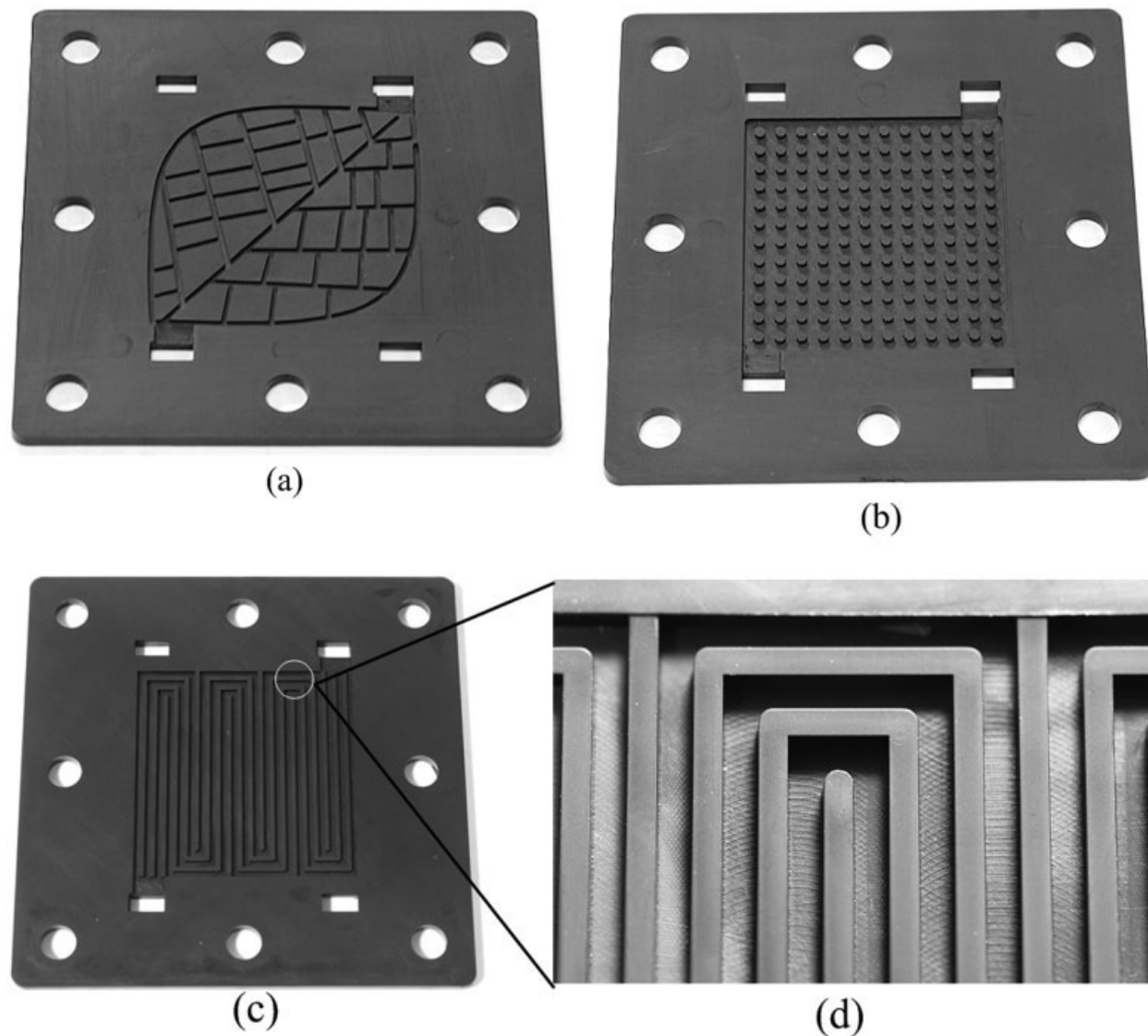
Figure 2 Injection-molded bipolar plates with: (a) branch, (b) grid, and (c) serpentine-type gas flow channels. (d) Magnified view of serpentine type channel.

influence of lead and other parasitic resistances can be neglected because the four-wire system used for measurement purposes in this study eliminates these resistances by comparing the voltage drop across the sample with the value of a defined reference element. To minimize the contact resistance, the copper collection current plates were sanded and polished before any measurements were taken. The measured through-plane resistance R_{meas} is given by:

$$R_{meas} = \frac{2R_{contact} + R_{bulk}}{A} \qquad (1)$$

where R_{meas} is measured through-plane resistance/Ω, $R_{contact}$ is contact resistance plate/media/Ω cm^2, R_{bulk}

is bulk through-plane resistance/Ω cm^2, and A is bipolar plate area/cm^2.

Note that with the exception of the bipolar plate area, the values above depend on the applied pressure.

RESULTS AND DISCUSSION

The optimal design of the flow channel configuration depends on the particular operational and environmental conditions. In this study, fuel cells were fabricated using three different flow-field plates (i.e., serpentine, grid, and branch). As discussed above, the performance of the three fuel cells was assessed by measuring the OCV and the maximum power density under a constant feed rate of the two reactants.
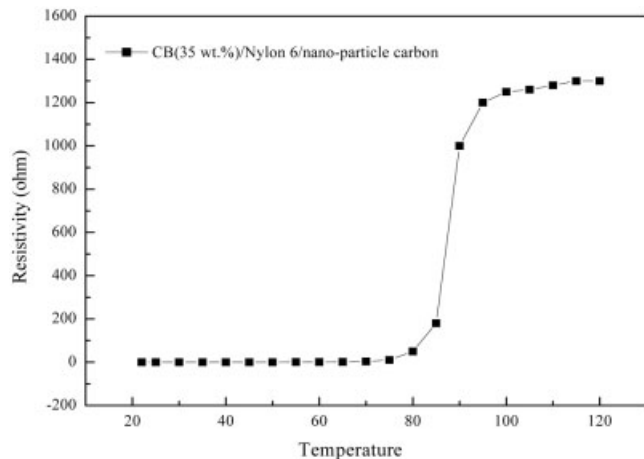
Figure 3 Variation of bipolar plate resistivity with temperature of CB/Nylon composite. Note that resistivity improves rapidly when temperature exceeds 90°C.

Figure 4 SEM image of carbon black and nanoparticle carbon-filled Nylon 6 blend.

Polymeric composite component heat temperature properties

The electrical properties of the present polymer composite were measured under temperatures of 22–120°C. As shown in Figure 3, when the temperature exceeds 90°C, the conductivity of the polymeric composite falls rapidly. At temperatures higher than 120°C, the resistance is very high and protects the polymeric composite cell.

Influence of polymeric composite compound carbon black on electric conductivity

At room temperature (25°C), the resistance reduces with increasing carbon black addition, as shown in Table IV. Nylon 6 is a nonconductive material. Although the addition of carbon black increases the conductivity, gaps still remain between the Nylon 6 and the carbon black elements. Therefore, the addition of carbon nanoparticles is necessary to ensure the maximum improvement in conductivity. Through trial and error, this study established that a carbon black addition of 35 wt % with a nanoparticle carbon addition of

10 wt % provided the optimum improvement in conductivity.

The SEM images (shown in Figs. 4 and 5) show the microstructure of the carbon black/Nylon 6/nanoparticle carbon (ϕ 30 nm) composite. The bulk resistance of the bipolar plate was measured with a four-point probe method. From Table IV, it can be seen that the electric bulk resistance of the composite material is 1.20 mΩ (conductivity 11.67 S/cm) for a carbon black addition of 35 wt % and a nanoparticle carbon addition of 10 wt %.

Performance testing of PEMFC

The nature of the reaction between the two reactants is determined by the shape of the gas flow channel. In other words, the gas flow channel configuration influences the efficiency of the PEM fuel cell. During performance testing, forced convection of the reactants (H_2 and O_2) into the catalyst layer was performed. Testing was performed at room temperature (25°C) and pressure (1 atm) with mass flow rates of the H_2 and O_2 reactants of 200 sccm, as shown in Table V.
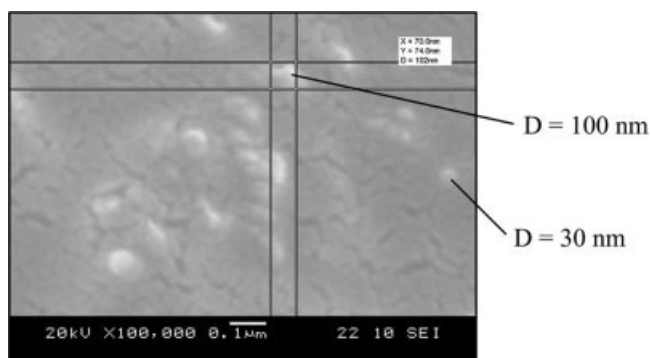

Figure 5 High magnification SEM image showing dimensions of carbon black (100–600 nm) and nanoparticle carbon (30–50 nm).

TABLE IV
Bulk Resistance and Conductivity of Carbon Black/Nylon6/Nanoparticle Carbon (10 wt %) Composite for Various CB Additions

Property	CB			
	20 wt %	25 wt %	30 wt %	35 wt %
Bulk resistance (Ω)	120	10	0.01	0.0012
Conductivity (S/cm)	1.17×10^{-4}	1.4×10^{-3}	1.4	11.67

TABLE V
Bipolar Plate Test Conditions

Condition	Value
Reaction area	$25\ cm^2$
Temperature	$25°C$
Anode and cathode side pressure	1 atm
Channel depth	1.5 mm
Channel width	1.2 mm
Rib width	1.5 mm
Bipolar plate thickness	3.5 mm
Mass flow rate (anode)	200 sccm
Mass flow rate (cathode)	200 sccm
Catalyst layer thickness (anode)	0.018 mm
Catalyst layer thickness (cathode)	0.026 mm
Diffuser layer thickness	0.2 mm

Note that during operation, the temperature of the cell does not exceed 55°C.

In the OCV tests, a maximum value of 0.97 V was obtained for the serpentine-type fuel cell (Fig. 6). The corresponding values for the serpentine-type, grid-type, and branch-type fuel cells were 0.94, 0.97, and 0.89 V [Figs. 7(a–c)], respectively. Since the reaction of the hydrogen and oxygen gases is rapid in the grid-type fuel cell, there is a smaller OCV than serpentine-type and branch-type fuel cells. This differs from the current ranges observed in standard fuel cells, which have a rapid initial fall of potential due to their electrochemical activation processes followed by ohmic polarization, in which an approximately linear potential drop occurs with an increase in the current density. In the fuel cell with a serpentine channel, the gas diffusion phenomenon is slower and so the VI curve has a larger current range.

It is found that the serpentine-type fuel cell yields a maximum power density of 330 mW/cm^2 at 0.42 V and 790 mA/cm^2. [Fig. 7(a)]. Meanwhile, the maxi-
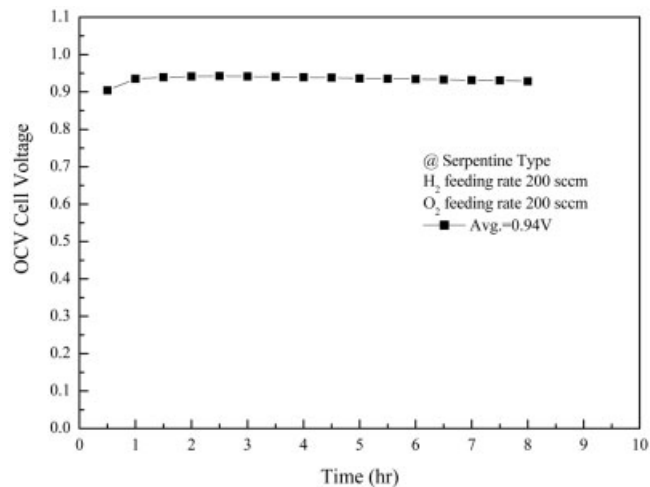

Figure 6 Variation of OCV over 8-h voltage test of bipolar plate with serpentine-type gas flow channel configuration.
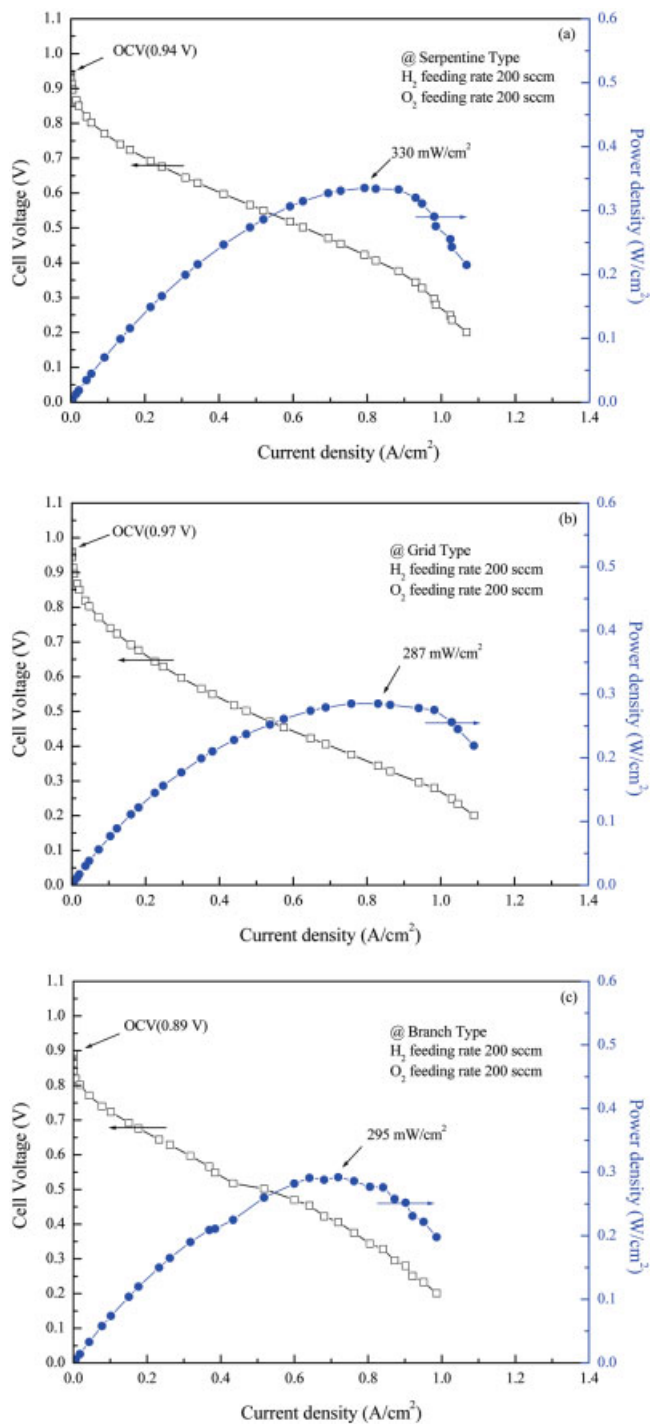

Figure 7 PEMFC characterization results for bipolar plates with different gas flow channel configurations. Variation of cell voltage and power density with current density for (a) serpentine, (b) grid, and (c) branch channel type fuel cells. [Color figure can be viewed in the online issue, which is available at www.interscience.wiley.com.]

mum power densities of the grid-type and branch-type fuel cells are found to be 287 mW/cm^2 at 0.35 V and 820 mA/cm^2 [Fig. 7(b)] and 295 mW/cm^2 at 0.41 V and 720 mA/cm^2 [Fig. 7(c)], respectively. From

these results, it is apparent that the serpentine-type fuel cell provides a better power density performance. The reason for this is that this gas flow channel configuration influences the forced convection in the membrane electrode assembly (MEA), postpones the gas reaction compared to the grid flow plate, and leads to a smoother draining of the water product. The improvement in the power density can be attributed primarily to the combined effects of a convective transport mechanism for the reactant gas together with a better distribution of the channels over the electrode area. Independent of the pressure drop, the increase in efficiency in the serpentine-type plate is directly related to the convective effect on the PEM fuel cell, which increases the amount of reagent which reaches the triple phase region where the reaction takes place. As shown in Table IV, the Nylon 6/carbon black (35 wt %) composite compound has the best electronic conductivity (11.67 S/cm) of the current compounds. However, increasing the carbon black content causes the composite to become stiff and brittle. Hence, fabricating the bipolar plates using an injection molding process is difficult. Improving the electronic conductivity of the bipolar plates, while simultaneously developing the means for their precision mass fabrication, is an important area of future research. With an operating voltage of 0.6 V, the fuel cells yielded a current density of 350 mA/cm^2 and a low power density of 210 mW/cm^2. Therefore, improving the current density is also an important future research topic.

CONCLUSIONS

This study has used Nylon 6, carbon black, and nano-particle carbon compounds to mold conductive plastic plates to replace the graphite plates traditionally used in PEM fuel cells. Polymeric composites are inexpensive, have favorable corrosive, hardness, and gas tightness properties, are lightweight and small, and are easy to manufacture.

Although the injection molding process offers many advantages, including the potential for automated production, short cycle times, precise tolerances, the bipolar plates fabricated using this process have the thickness ratio of optimization, can not be operated at temperatures greater than 120°C, and lead to a poor conductivity of the PEM fuel cells stack.

Concerning the electric conduction characteristics of the PEM fuel cell, an improvement has been observed when the present bipolar plates are used. However, it is important to investigate, over the long term, the trend of this increment and its influence on the power efficiency of the PEM fuel cell.

References

1. Davies, D. P.; Adcock, P. L.; Turpin M. T.; Rowen, S. J. J Appl Electrochem 2000, 30, 101.
2. Scholta, J.; Rohland, B.; Trapp, V.; Focken, U. J Power Sources 1999, 84, 231.
3. Bar-On, I.; Kirchain, R.; Roth, R. J Power Sources 2002, 109, 71.
4. Vielstich, W.; Lamm, A.; Gasteiger, H. A. Handbook of Fuel Cells: Fundamentals Technology and Applications; Wiley: England, 2003; Vol.3, p 286.
5. Hornung, R.; Kappelt, G. J Power Sources 1998, 72, 20.
6. Hentall, P. L.; Lakeman, J. B.; Mepsted, G. O.; Adcock, P. L.; Moore, J. M. J Power Sources 1999, 80, 235.
7. Makkus, R. C.; Janssen, A. H. H.; Bruijn, F. A.; Mallant, R. K. A. M. J Power Sources 2000, 86, 274.
8. Rio, C. D.; Ojeda, M. C.; Acosta, J. L.; Escudero, M. J.; Homtanon, E.; Daza, L. J Appl Polym Sci 2002, 83, 2817.
9. Besmann, T. M.; Klett, J. W.; Henry, J. J.; Lara-Curzio, E. J Electrochem Soc 2000, 147, 4083.
10. Wu, M.; Shaw, L. L. J Power Sources 2004, 136, 37.
11. Mighri, F.; Huneault, M. A.; Champagne, M. F. Polym Eng Sci 2004, 44, 9.
12. Che, G.; Lakshmi, B. B.; Martin, C. R.; Fisher, E. R.; Ruoff, R. S. Chem Mater 1998, 10, 260.
13. Che, G.; Lakshmi, B. B.; Fisher, E. R.; Martin, C. R. Nature 1998, 393, 346.
14. Zhang, M. Q.; Xu, J. R.; Zeng, H. M.; Huo, Q.; Zhang, Z. Y.; Yun, F. C.; Friendrich, K. J Mater Sci 1995, 30, 4226.
15. Lux, F. Polym Eng Sci 1993, 33, 334.
16. Asai, S.; Sumita, M. J Macromol Sci Phys 1995, 34, 283.
17. AL-Allak, H. M.; Brinkman, A. W.; Woods, J. J Mater Sci 1993, 28, 117.
18. Heaney, M. B. Appl Phys Lett 1996, 69, 2602.
19. Yu, G.; Zhang, M. Q.; Zeng, H. M. J Appl Polym Sci 1998, 70, 559.